JOURNAL OF AGRICULTURAL AND FOOD CHEMISTRY

Affinity and Rate Constants for Interactions of Bovine Folate-Binding Protein and Folate Derivatives Determined by Optical Biosensor Technology. Effect of Stereoselectivity

LINNÉA NYGREN-BABOL, ÅSE STERNESJÖ, MARGARETA JÄGERSTAD, AND LENNART BJÖRCK*

Department of Food Science, Swedish University of Agricultural Sciences, SE-750 07 Uppsala, Sweden

The interactions between bovine folate-binding protein (FBP) and different folate derivatives in pure diastereoisomeric forms were studied at pH 7.4 by a surface plasmon resonance technology (Biacore). The results show that folic acid had the most rapid association rate ($k_a = 1.0 \times 10^6$ M^{-1} s^{-1}), whereas (6*S*)-5-HCO-5,6,7,8-tetrahydrofolic acid had the most rapid dissociation rate ($k_d = 3.2 \times 10^{-3}$ s^{-1}). The equilibrium dissociation constant (K_D), calculated from the quotient of k_d/k_a, showed that the two forms of folates not occurring in nature, that is, folic acid and (6*R*)-5-CH_3-5,6,7,8-tetrahydrofolic acid, had the highest affinities for FBP, 20 and 160 pmol/L, respectively. The results thus show that there were great differences in the interactions between folate-binding protein and the major forms of folate derivatives. The nutritional implications of these differences are discussed.

KEYWORDS: Folate-binding protein; optical biosensor; rate constant; equilibrium constant; folic acid; 5-methyltetrahydrofolate diastereomers

INTRODUCTION

Folates are a group of water-soluble B-vitamins, which are essential for the transfer of one-carbon units in the synthesis of DNA and certain amino acids, for example, methionine from homocysteine. An optimal folate status in humans is linked to several health benefits including reduced risk of neural tube defects in fetus, cardiovascular diseases caused by increased plasma homocystine levels, and certain cancer forms (*1*). Chemically, folate consists of a pteridine ring attached to a *p*-aminobenzoate, which in turn is linked to L-glutamate (**Figure 1**). The pteridine ring of pteroyl-L-glutamic acid (PteGlu) is fully oxidized and exists in nature in only trace quantities. The majority of naturally occurring forms of folate in plants, animals, and microorganisms are fully reduced 5,6,7,8-tetrahydrofolates (H_4folate), with or without one-carbon substituents, predominantly methyl or formyl groups, linked at the N^5- and/or N^{10}-position (*2*). All fully reduced folates have two chiral centers, that is, at the α-C atom in the glutamic acid moiety and at the C-atom in position 6 (C6) of the pteroyl moiety (*3*). C6 in the pteridine ring is a tetrahedral stereocenter, and all H_4folate forms therefore exist in either the *R* or *S* configuration. To exhibit vitamin activity the C6 in the pteridine ring and the glutamic acid part of the H_4folate molecule must be in the *S* configuration. Most of the naturally occurring folates have a side chain of 3−11 glutamate residues (*S* configuration) with γ-peptide linkage (*4*).

Absorption and cellular uptake of folates is mediated by two different classes of membrane proteins (*5*). One class consists of the reduced folate carriers (RFCs), which are transmembrane proteins that bind reduced folate with a micromolar affinity. The other is the family of folate-binding proteins (FBP), which exist both as membrane-associated (GPI anchored) folate receptors and as soluble forms in milk and other body fluids (*6*). This latter protein family shares biochemical and molecular properties, but the different proteins are encoded by independent genes that are expressed in a restricted, independent, and tissue-specific manner. The effects that these different FBP forms exert on folate stability, bioavailability, and homeostasis is not well understood; the differences in their binding properties might be important.

The high intake of bovine milk in many countries makes the nutritional impact of FBP interesting, because FBP might bind folates from other dietary sources and through this may influence folate bioavailability. Recently published data indicate that FBP might have an inhibitory effect on the bioavailability of the synthetic folic acid (PteGlu) (*7*). Bovine FBP is also widely used in clinical methods such as the competitive binding assay (RPBA) for the analysis of folate status (serum folate, red blood cell folate, whole blood folate). Moreover, affinity chromatography based on FBP is commonly used for purification of samples prior to HPLC analysis of natural folates in foods (*8*−*11*). For both of these applications of FBP, the binding characteristics are of utmost importance. To our knowledge there are no published data on equilibrium constants for H_4folate derivatives binding to bovine FBP. Because pure *S*- and

* Address correspondence to this author at the Department of Food Science, Swedish University of Agricultural Sciences (SLU), P.O. Box 7051, SE-750 07 Uppsala, Sweden [e-mail Lennart.Bjorck@lmv.slu.se; telephone +46 (0)18 67 2039; fax +46(0)18 67 29 95].

10.1021/jf058017u CCC: $30.25
Published on Web 06/04/2005

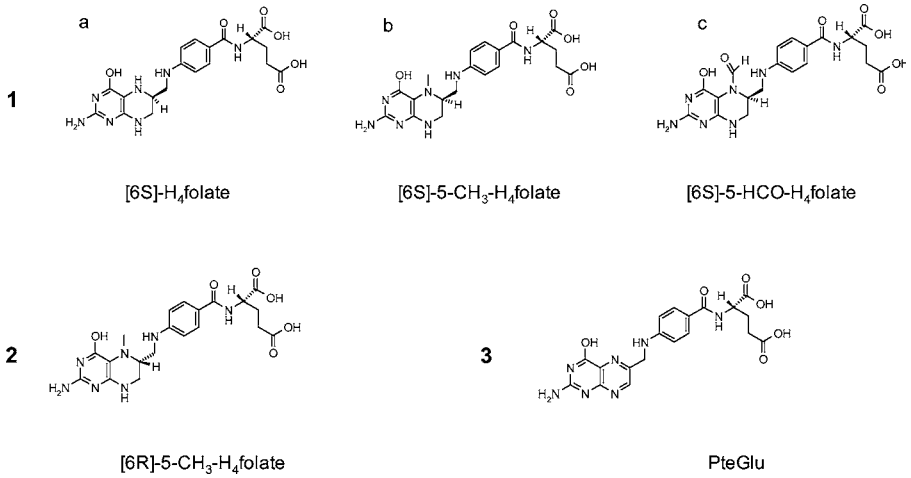

Figure 1. Chemical structures of folate derivatives studied: (**1**) 6*S*-isomers; (**2**) 6*R*-isomer; (**3**) PteGlu.

R-diastereoisomers of C6 now are available, it has become possible to investigate the differences in binding properties between these two forms.

We have utilized a surface plasmon resonance (SPR) biosensor technology (Biacore) to study the interaction between different derivatives and C6 diastereoisomers of folates with bovine FBP. The assay is based on our previously developed method for the determination of FBP in bovine milk (*12*, *13*), and in this paper we present affinity and kinetic data relating to the interaction between bovine folate-binding protein and the most common folate derivatives in pure diastereoisomeric forms.

MATERIALS AND METHODS

Materials. FBP was purified from bovine milk as previously described (*12*). The reduced forms of the monoglutamic folates (6*S*)-5,6,7,8-tetrahydrofolic acid sodium salt [(6*S*)-H_4folate], (6*S*)-5-HCO-5,6,7,8-tetrahydrofolic acid sodium salt [(6*S*)-5-HCO-H_4folate], (6*S*)-5-CH_3-5,6,7,8-tetrahydrofolic acid sodium salt [(6*S*)-5-CH_3-H_4folate], and (6*R*)-5-CH_3-5,6,7,8-tetrahydrofolic acid sodium salt [(6*R*)-5-CH_3-H_4folate] were kindly donated by Merck Eprova AG (Schaffhausen, Switzerland) and stored at −80 °C until use. Folic acid (pteroyl-L-glutamic acid, PteGlu) was obtained from Sigma Chemical Co. (St. Louis, MO). The chemical structures are summarized in **Figure 1**.

A Biacore 1000 instrument was used for surface plasmon resonance analysis, and a BiacoreQ instrument with an external surface preparative unit was used for immobilization of the folates. Sensor Chip CM5 (research grade), HBS-EP buffer, pH 7.4 [10 mmol/L 4-(2-hydroxyethyl)piperazine-1-ethanesulfonic acid (HEPES), 3.0 mmol/L EDTA, 150 mmol/L NaCl, 0.005% (v/v) surfactant P-20], and amine coupling kit [*N*-ethyl-*N*′-(3-ethylaminopropyl)carbodiimide (EDC), *N*-hydroxysuccinimide (NHS), and ethanolamine hydrochloride] were obtained from Biacore AB (Uppsala, Sweden).

Because the amine group of folates is essential for the binding to FBP (*12*), direct amine coupling to the activated dextran is not an option. Instead, folates were converted to their hydroxysuccinimidyl derivative and coupled to amino groups on the surface. To obtain low-density surfaces, the CM5 sensor chip was activated with a 3-min injection of 0.05 mol/L NHS and 0.2 mol/L EDC, followed by a 3-min injection of 100 mmol/L ethylenediamine, dissolved in 50 mmol/L borate buffer, pH 8.5, to attach amino groups onto the chip. The remaining binding sites were blocked with 1.0 mol/L ethanolamine, pH 8.5, for 3 min. Equal volumes of 0.05 mol/L NHS and 0.2 mol/L EDC were mixed and diluted 5:1 with 6 mmol/L folate dissolved in 50 mmol/L borate buffer, pH 8.5, and incubated for 20 min at room temperature. After incubation, the solution was mixed with an equal volume of 50 mmol/L borate buffer, pH 8.5, and injected for 3 min to immobilize the folates to the sensor surface. Making high-density surfaces followed the same procedure but with 7-min injections of NHS/EDC and the hydroxysuccinimidyl derivative of PteGlu. Reference surfaces were activated and blocked as outlined above for subtraction of nonspecific binding and instrument noise. The coupling procedures were performed at a flow rate of 5 μL/min at 25 °C.

Kinetic Analysis of FBP/Folate Interactions. For collection of detailed kinetic data, concentration series of FBP were injected over the different folate surfaces at a flow rate of 60 μL/min. Concentrations of 3, 6, 12, and 24 nmol/L were injected for 240 s, and dissociation was monitored for 400 s for (6*S*)-5-HCO-H_4folate and (6*S*)-5-CH_3-H_4-folate. Concentrations of 1.5, 3, 6, and 12 nmol/L were injected for 240 s, and dissociation was monitored for 480 s for (6*S*)-5-H_4folate. Concentrations of 3, 6, 12, and 24 nmol/L were injected for 240 s, and dissociation was monitored for 600 s for (6*R*)-5-CH_3-H_4folate. Concentrations of 0.375, 0.75, 1.5, 3, and 6 nmol/L were injected for 240 s, and dissociation was monitored for 1920 s for PteGlu. All binding experiments were carried out with HBS-EP running buffer, pH 7.4, at 25 °C, and each concentration was injected in triplicate using random order.

Estimation of Rate and Equilibrium Constants. Kinetic analyses of biosensor data were performed as outlined by O'Shannessy and Winzor (*14*), and a brief review is presented below. A biomolecular interaction between a soluble analyte (A) and an immobilized ligand (X) can be interpreted by pseudo-first-order kinetics under the setting in the Biacore and may be described by the equation

$$A + X \underset{k_d}{\overset{k_a}{\leftrightarrow}} AX$$

where k_a and k_d are the respective association and dissociation rate constants, and ratio of k_a over k_d describes the equilibrium dissociation constant (K_D). The rate of formation of complex is described by the differential equation (*15*)

$$\frac{dC_{Ax}}{dt} = k_a(C_A)_i[(C_x)_{tot} - (C_{Ax})_t] - k_d(C_{Ax})_t \qquad (1)$$

where C_{Ax} is the molar concentration of complex at the sensor surface, $(C_A)_i$ is the concentration of analyte injected and maintained over the sensor surface, $(C_x)_{tot}$ is the concentration of immobilized ligand, and $(C_{Ax})_t$ is the concentration of complex at the sensor surface at time *t*. When flow-cell-based biosensor analysis is employed, eq 1 can be rewritten and integrated to give the following association rate equation for the 1:1 pseudo-first-order interaction.

$$R_t = \frac{k_a(C_A)_i R_{max}(1 - \exp[-k_a(C_A)_i + k_d]t)}{k_a(C_A)_i + k_d} \qquad (2)$$

where R_{max} is the maximum response if all available ligand binding sites are occupied and R_t is the biosensor response at time *t*. The pseudo-

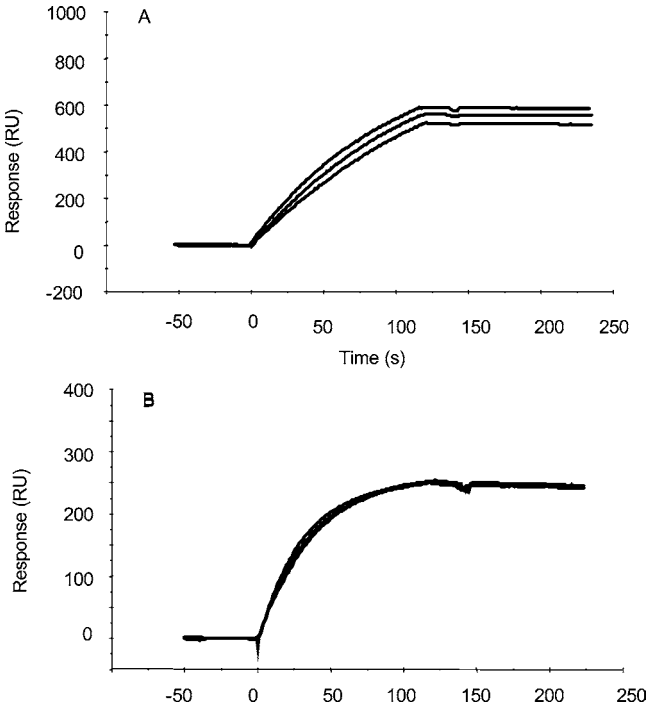

Figure 2. Sensorgrams of FBP (30 nmol/L) injected over a PteGlu surface at flow rates of 60, 30, and 15 μL/min: (**A**) high ligand density surface (the increase in binding rate with increasing flow rate is an indication that this surface is affected by mass transport); (**B**) low ligand density surface (no increase in binding rates).

first-order dissociation phase is described by the equation

$$R_t = R_0 \exp(-k_d t) \quad (3)$$

where R_0 is the response at the start of the dissociation phase.

Data Processing and Analysis. Double referencing was used to process the triplicate injection data of each concentration. The binding response observed was adjusted by subtracting the response observed with a representative reference surface and blank injection (*16*). To obtain kinetic rate constants, adjusted response data were then fitted with nonlinear least-squares regression analysis (BIA evaluation 3.0 software), and the curve was accepted if it fulfilled the following criteria: acceptable overlay and residual plots, χ_2 value <4, and T value >10. R_{max} was obtained by repeated injections of high analyte concentrations to saturate the sensor surface. The data were globally fitted to a simple interaction model (A + B = AB) except for the (6*R*)-5-CH_3-H_4folate data, where R_{max} was set as a local parameter because of the instability of the ligand. The equilibrium dissociation constant (K_D) was determined by the quotient of k_d/k_a. Constants reported represent the average of three independent analyses of each FBP/folate interaction.

RESULTS

Direct binding of FBP to immobilized folate surfaces was studied to determine kinetic rate constants. To exclude mass transport limitation, low ligand density surfaces were prepared by reducing the injection volumes during activation and immobilization of the surface. This proved to be adequate for excluding mass transport limitation (**Figure 2**). The sensorgrams in **Figure 3** show representative overlay plots of triplicate injections of concentration series with FBP. Each of the binding responses shown was well described by a 1:1 interaction model. Considerable differences were found for both association rate constants (k_a) and dissociation rate constants (k_d) between the different folate forms (**Table 1**). PteGlu exhibited the most rapid

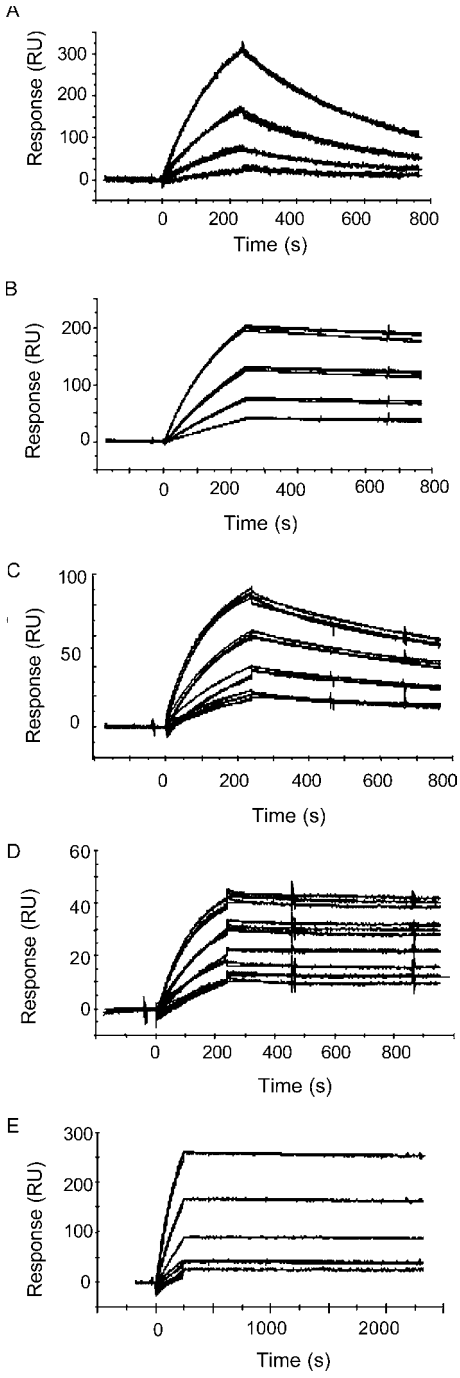

Figure 3. Sensorgrams of triplicate injections of FBP globally fitted to a 1:1 biomolecular interaction model: (**A**) (6*S*)-5-HCO-H_4folate was injected at concentrations of 3, 6, 12, and 24 nmol/L for 240 s, and dissociation was monitored for 400 s; (**B**) (6*S*)-H_4folate was injected at concentrations of 1.5, 3, 6, and 12 nmol/L for 240 s, and dissociation was monitored for 480 s; (**C**) (6*S*)-5-CH_3-H_4folate was injected at concentrations of 3, 6, 12, and 24 nmol/L for 240 s, and dissociation was monitored for 400 s; (**D**) (6*R*)-5-CH_3-H_4folate was injected at concentrations of 3, 6, 12, and 24 nmol/L for 240 s, and dissociation was monitored for 600 s; (**E**) PteGlu was injected at concentrations of 0.375, 0.75, 1.5, 3, and 6 nmol/L for 240 s, and dissociation was monitored for 1920 s.

association rate constant and (6*S*)-5-HCO-H_4folate the most rapid dissociation rate constant.

The equilibrium dissociation constant (K_D) (**Table 1**) showed that the two folate forms that do not occur in nature, namely, PteGlu and (6*R*)-5-CH_3-H_4folate, had the highest affinities for FBP, 20 and 160 pmol/L, respectively. Among the naturally

Table 1. Affinity and Rate Constants of FBP/Folate Interaction[a]

folate	K_a (M^{-1} s^{-1})	K_d (s^{-1})	K_D (pM)
PteGlu	$(1.0 \pm 0.4) \times 10^6$	$(1.3 \pm 0.4) \times 10^{-5}$	20 ± 9
(6*R*)-5-CH_3-H_4folate	$(3.0 \pm 0.4) \times 10^5$	$(4.7 \pm 1.7) \times 10^{-5}$	160 ± 50
(6*S*)-H_4folate	$(3.8 \pm 0.3) \times 10^5$	$(9.7 \pm 3.0) \times 10^{-5}$	250 ± 60
(6*S*)-5-CH_3-H_4folate	$(2.8 \pm 0.3) \times 10^5$	$(5.7 \pm 1.0) \times 10^{-4}$	2000 ± 200
(6*S*)-5-HCO-H_4folate	$(1.2 \pm 0.2) \times 10^5$	$(3.2 \pm 1.0) \times 10^{-3}$	12000 ± 3000

[a] Mean values ± standard error obtained from three or more independent measurements on different surfaces.

occurring folates, (6*S*)-H_4folate had the highest affinity (250 pmol/L), (6*S*)-5-CH_3-H_4folate almost 10-fold lower (2000 pmol/L), and (6*S*)-5-HCO-H_4folate the lowest affinity of all (12000 pmol/L).

There were some differences in the response between the triplicate injections of the same concentration of (6*R*)-5-CH_3-H_4folate (**Figure 3D**). This was due to a decrease of ligand density at the sensor surface and was caused by degradation of (6*R*)-5-CH_3-H_4folate. Therefore, when the sensorgrams for 6*S*- and 6*R*-stereoisomers of 5-CH_3-H_4folate are compared, it is clearly seen that the 6*S* form was more stable under the conditions described. The naturally occurring 6*S* form of 5-CH_3-H_4folate was also subject to degradation on the sensor surface, but not to an extent to affect the assay. Our experience is that the order of stability for the naturally existing 6*S* forms is (6*S*)-5-CH_3-H_4folate ≥ (6*S*)-5-HCO-H_4folate > (6*S*)-H_4folate under the conditions used in the Biacore. In contrast, the PteGlu surfaces were very stable, and no decrease in response was observed.

DISCUSSION

In contrast to many previous studies, our model allows studies of affinity and dissociation rate constants of the binding characteristics of bovine FBP and different folate forms in real time. The results presented show that there are essential differences in binding characteristics between FBP and the different folate forms as well as between C6 diastereoisomers of 5-CH_3-H_4folate. The H_4folate molecules have at least two stereocenters, and the 6*R* and 6*S* forms are not enantiomeric because the glutamic acid moiety is in the *S* configuration (L-glutamic acid). They are thus not mirror images but two distinct molecules with different physical and chemical properties.

The results show that the order of affinity to FBP at pH 7.4 was PteGlu > (6*R*)-5-CH_3-H_4folate > (6*S*)-H_4folate > (6*S*)-5-CH_3-H_4folate > (6*S*)-5-HCO-H_4folate. Previous studies have shown similar differences in affinity among the folate forms (*17*−*19*) even though most of the previous studies are based on racemic mixtures and not the pure stereoisomeric forms of C6. Recently published affinity data (*20*) demonstrated an equilibrium dissociation constant (K_D) for PteGlu (20 pmol/L) at neutral pH equal to the findings in our study. These data were obtained by using centrifugal ultrafiltration−dialysis to quantify the binding of PteGlu to bovine FBP. The authors also discussed the possibility that previously reported equilibrium constants (*21*−*23*) obtained at neutral pH were not adequate because of the high protein concentrations used. We did not find any deviation from the 1:1 interaction model because no improvement was found when more complex models were used. It may, therefore, be assumed that the interaction obeyed a simple bimolecular model.

The 10-fold lower affinity of (6*S*)-5-CH_3-H_4folate compared with PteGlu found in the present study explains the impact of FBP on folate bioavailability from milk containing active FBP. Recently, bioaccessibility studies based on an in vitro model, simulating human gastric passage, reported lower ($p < 0.05$), sometimes only 50%, bioaccessibility of PteGlu compared with (6*S*)-5-CH_3-H_4folate (*24*). In these studies, either pasteurized milk or yogurt was fortified with either of these two folate forms with and without added FBP in equimolar amounts (*7*, *24*). Interestingly, previous work of these authors (*7*, *24*) also demonstrates partial (up to 34%) stability of FBP during the in vitro gastrointestinal passage simulating an adult human situation. This indicates that a larger portion of folic acid passed the gastrointestinal tract bound to FBP compared with (6*S*)-5-CH_3-H_4folate. For infants, a much higher survival of FBP could be expected due to a less matured gastrointestinal system; for example, the gastric pH is higher and an infant's intestinal mucosa is more permeable. This addresses questions for further elucidation: whether there exist ileal receptors for the FBP: folate complex, as suggested by some investigators (*25*), and, if so, are these receptors specific for human FBP only or also for bovine milk FBP? Future studies on infants are necessary as FBP forms a stable complex with folic acid as seen in previous (*7*, *24*, *26*) and present studies. Most infant formulas and gruels are fortified with PteGlu, and as these products nowadays are gently processed, active FBP might still be present and able to impair the folate bioavailability.

Another controversial issue that our affinity kinetic model might help to elucidate is whether folate-binding proteins are present in enterocytes or the brush-border of intestinal mucosa or in the liver of mammals as have been reported in some studies (*18*, *27*, *28*) but not in others. For instance, the brush-border from rat intestine and hog intestine has been reported to contain folate-binding proteins, whereas no corresponding data yet are available for humans (*18*). There are also some contradicting results on whether FBP is expressed in the liver or not. Two forms of FBP have been identified by gel filtration of Triton X-100 extracts of rat (*29*) and human (*30*) liver plasma membranes. On the other hand, FBP mRNA could not be found when Northern blots were performed in human and rat liver cell extracts (*31*). Better knowledge in this field will enable improved interpretation of bioavailability models and data for different folate forms, for example, oxidation status, polymerization/conjugation degree, and pure diastereoisomers or racemic mixtures, necessary for decision of the best form to be used for enrichment/fortification and supplemental purposes.

Today, competitive binding methods are routinely used for folate analysis of clinical samples (*32*, *33*). The principle of the competitive binding assay is based on competition between folates in the sample or standard and a known amount of labeled folate for the limited binding sites on a folate-binding protein from bovine milk. The most common standard is PteGlu because of its greater stability compared with native folates. At pH 9.3 the affinity of the FBP is shown to be equal for folic acid and the diastereoisomer mixture (6*R*,*S*)-5-CH_3-H_4folate (*34*). The dominating folate form in plasma is, however, (6*S*)-5-CH_3-H_4-folate, a form that has become commercially available first during recent years. When Waxman and co-workers (*35*) introduced the competitive protein binding assay for the measurement of serum folate levels more than 30 years ago, they used a non-radioactive racemic mixture of 5-CH_3-H_4folate as standard and the (6*S*)-stereoisomer of radioactive (^{3}H)5-CH_3-H_4folate as competitive radioactive folate. Waxman and co-workers conclude from their results that only the active (6*S*)-5-CH_3-H_4folate isomer binds to FBP. Moreover, they clearly show that neither folinic acid (5-CHO-H_4folate) nor methotrexate binds to bovine FBP. Furthermore, Shane's group (*17*),

10 years later, report relative activities of purified folate standards using in-house-synthesized racemic mixtures and pure stereoisomers. These folate derivatives are tested in four different commercial radioassay kits of which two are based on bovine FBP. Shane and co-workers find only small differences (<5%) in relative activities between PteGlu, (6*S*)-5-CH_3-H_4folate and (6*R*,*S*)-5-CH_3-H_4folate for one kit (Bio-Rad). The kit of Schwarz-Mann, on the other hand, shows the following relative activities: PteGlu (0.93), (6*S*)-5-CH_3-H_4folate (1.00), and (6*R*,*S*)-5-CH_3-H_4folate (1.27), indicating ~30% difference between certain folate derivatives. One explanation for these differences given by the authors is that the commercial assay kits differ in type of diluting system, either buffer, serum, or human serum albumin is used, which might influence the result. However, a modified competitive binding assay has recently been developed and evaluated for folate analysis of food samples (*19*). Studies of the responses for different folate derivatives in this modified assay show the following response factors in decreasing order: (6*S*)-H_4folate > PteGlu > (6*R*,*S*)-CH_3-H_4folate > (6*S*)-CH_3-H_4folate > HCHO-H_4folate. The (6*R*,*S*)-5-CH_3-H_4folate along with PteGlu show ~30% stronger response in the assay compared with the biologically active (6*S*)-5-CH_3-H_4folate. These findings are clearly supported by the data for different folate forms reported in the present study and imply that there is an urgent need to calibrate clinical binding assays based on FBP for PteGlu and (6*S*)-5-CH_3-H_4folate instead of standards used hitherto, for example, PteGlu and (6*R*,*S*)-5-CH_3-H_4folate. A consequence of this might well be different cutoff levels for deficient, marginal, and normal folate concentrations in clinical samples compared with currently used values.

In conclusion, this is the first study that has investigated binding interactions between FBP and pure stereoisomeric forms of various folates based on real time monitoring of affinity and dissociation rates quantified by an optical biosensor technology. It demonstrates that there were marked differences in binding properties between different folates, which is of importance in understanding their bioavailability and metabolism. The high resolution of surface plasmon resonance methodology might also provide new possibilities to study binding characteristics of other bioactive substances in foods, which, in combination with nutrition studies, would promote new knowledge in the field of food science and nutrition.

ACKNOWLEDGMENT

We gratefully thank Dr. C. Witthöft and Dr. J. Jastrebova for valuable discussions and advice during the study.

LITERATURE CITED

(1) Selhub, J.; Rosenberg, I. H. *Present Knowledge in Nutrition*; Ziegler, E. E., Filer, L. J., Eds.; ILSI Press: Washington, DC, 1996; pp 206−219.

(2) Blakley, R. L. Nomenclature and symbols for folic acid and related compounds. *J. Biol. Chem.* **1988**, *263*, 605−607.

(3) Groehn, T.; Moser, R., Synthesis of optically pure diastereoisomers of reduced folates. *Pteridines* **1999**, *10*, 95−100.

(4) Scott, J.; Rébeille, F.; Fletcher, J. Folic acid and folates: the feasibility for nutritional enhancement in plant food. *J. Sci. Food Agric.* **2000**, *80*, 795−824.

(5) Brzezinska, A.; Winska, P.; Balinska, M. Cellular aspects of folate and antifolate membrane transport. *Acta Biochim. Pol.* **2000**, *47*, 735−749.

(6) Elnakat, H.; Ratnam, M. Distribution, functionality and gene regulation of folate receptor isoforms: implications in targeted therapy. *Adv. Drug Deliv. Rev.* **2004**, *56*, 1067−1084.

(7) Arkbåge, K.; Verwei, M.; Havenaar, R.; Witthoft, C. Bioaccessibility of folic acid and (6*S*)-5-methyltetrahydrofolate decreases after the addition of folate-binding protein to yogurt as studied in a dynamic in vitro gastrointestinal model. *J. Nutr.* **2003**, *133*, 3678−3683.

(8) Selhub, J. Determination of tissue folate composition by affinity chromatography followed by high-pressure ion pair liquid chromatography. *Anal. Biochem.* **1989**, *182*, 84−93.

(9) Konings, E. J. A validated liquid chromatographic method for determining folates in vegetables, milk powder, liver, and flour. *J. AOAC Int.* **1999**, *82*, 119−127.

(10) Kariluoto, S.; Vahteristo, L. T.; Piironen, V. Applicability of microbiological assay and affinity chromatography purification followed by high-performance liquid chromatography (HPLC) in studying folate contents in rye. *J. Sci. Food Agric.* **2001**, *81*, 938−942.

(11) Witthoft, C.; Strålsjö, L.; Berglund, G.; Lundin, E. A human model to determine folate bioavailability from food—a pilot study for evaluation. *Scand. J. Nutr.* **2003**, *47*, 6−18.

(12) Nygren, L.; Sternesjö, Å.; Björck, L. Determination of folate-binding protein from milk by optical biosensor analysis. *Int. Dairy J.* **2003**, *13*, 283−290.

(13) Nygren-Babol, L.; Sternesjö, Å.; Björck, L. Factors influencing levels of folate-binding protein in bovine milk. *Int. Dairy J.* **2004**, *14*, 761−765.

(14) O'Shannessy, D. J.; Winzor, D. J. Interpretation of deviations from pseudo-first-order kinetic behavior in the characterization of ligand binding by biosensor technology. *Anal. Biochem.* **1996**, *236*, 275−83.

(15) Fägerstam, L. G.; O'Shannessy, D. J. *Handbook of Affinity Chromatography*; Kline, T., Ed.; Dekker: New York, 1993; Vol. 63, pp 229−252.

(16) Myszka, D. G. Improving biosensor analysis. *J. Mol. Recognit.* **1999**, *12*, 279−284.

(17) Shane, B.; Tamura, T.; Stokstad, E. L. Folate assay: a comparison of radioassay and microbiological methods. *Clin. Chim. Acta* **1980**, *100*, 13−19.

(18) Kane, M.; Waxman, S. Biology of disease. Role of folate binding protein in folate metabolism. *Lab. Invest.* **1989**, *60*, 736−746.

(19) Strålsjö, L.; Arkbage, K.; Witthoft, C.; Jägerstad, M. Evaluation of a radioprotein-binding assay (RPBA) for folate analysis in berries and milk. *Food Chem.* **2002**, *79*, 525−534.

(20) Nixon, P. F.; Jones, M.; Winzor, D. J. Quantitative description of the interaction between folate and the folate-binding protein from cow's milk. *Biochem. J.* **2004**, *382*, 215−221.

(21) Salter, D. N.; Scott, K. J.; Slade, H.; Andrews, P. The preparation and properties of folate-binding protein from cow's milk. *Biochem. J.* **1981**, *193*, 469−476.

(22) Hansen, S. I.; Holm, J.; Lyngbye, J. Cooperative binding of folate to a protein isolated from cow's whey. *Biochim. Biophys. Acta* **1978**, *535*, 309−318.

(23) Hansen, S. I.; Holm, J.; Lyngbye, J.; Pedersen, T. G.; Svendsen, I. Dependence of aggregation and ligand affinity on the concentration of the folate-binding protein from cow's milk. *Arch. Biochem. Biophys.* **1983**, *226*, 636−642.

(24) Verwei, M.; Arkbage, K.; Mocking, H.; Havenaar, R.; Groten, J. The binding of folic acid and 5-methyltetrahydrofolate to folate-binding proteins during gastric passage differs in a dynamic in vitro gastrointestinal model. *J. Nutr.* **2004**, *134*, 31−37.

(25) Selhub, J.; Dhar, G. J.; Rosenberg, I. H. Gastrointestinal absorption of folates and antifolates. *Pharmacol. Ther.* **1983**, *20*, 397−418.

(26) Verwei, M.; Arkbage, K.; Havenaar, R.; van den Berg, H.; Witthoft, C.; Schaafsma, G. Folic acid and 5-methyltetrahydrofolate in fortified milk are bioaccessible as determined in a dynamic in vitro gastrointestinal model. *J. Nutr.* **2003**, *133*, 2377−2383.

(27) Wagner, K. Folate-binding proteins. *Nutr. Rev.* **1985**, *43*, 293−299.

(28) Parodi, P. W. Cow's milk folate binding protein: Its role in folate nutrition. *Aust. J. Dairy Technol*. **1997**, *52*, 109−118.
(29) da Costa, M.; Rothenberg, S. P. Characterization of the folate-binding proteins associated with the plasma membrane of rat liver. *Biochim. Biophys. Acta* **1988**, *939*, 533−541.
(30) Holm, J.; Hansen, S. I.; Hoier-Madsen, M. High-affinity folate binding in human liver membranes. *Biosci. Rep*. **1991**, *11*, 139−145.
(31) Villanueva, J.; Ling, E. H.; Chandler, C. J.; Halsted, C. H. Membrane and tissue distribution of folate binding protein in pig. *Am. J. Physiol*. **1998**, *275*, R1503−R1510.
(32) van den Berg, H.; Finglas, P. M.; Bates, C. FLAIR intercomparisons on serum and red cell folate. *Int. J. Vitam. Nutr. Res*. **1994**, *64*, 288−293.
(33) Raiten, D. J.; Fisher, K. D. Assessment of folate methodology used in the Third National Health and Nutrition Examination Survey (NHANES III, 1988−1994). *J. Nutr*. **1995**, *125*, 1371S−1398S.
(34) Givas, J. K.; Gutcho, S. pH dependence of the binding of folates to milk binder in radioassay of folates. *Clin. Chem*. **1975**, *21*, 427−428.
(35) Waxman, S.; Schreiber, C.; Herbert, V. Radioisotopic assay for measurement of serum folate levels. *Blood* **1971**, *38*, 219−228.

Received for review January 7, 2005. Revised manuscript received April 21, 2005. Accepted May 5, 2005.

JF058017U